

Free vibration analysis of stiffened laminated plates using layered finite element method

Meiwen Guo[†]

Parsons Brinckerhoff, Inc., 510 First Avenue North, Suite 500, Minneapolis, MN 55403, USA

Issam E. Harik[‡]

Department of Civil Engineering, University of Kentucky, Lexington, KY 40506-0281, USA

Wei-Xin Ren^{‡†}

*Department of Civil Engineering, Fuzhou University, Fuzhou, Fujian Province 35002
People's Republic of China*

(Received March 28, 2001, Accepted July 9, 2002)

Abstract. The free vibration analysis of stiffened laminated composite plates has been performed using the layered (zigzag) finite element method based on the first order shear deformation theory. The layers of the laminated plate is modeled using nine-node isoparametric degenerated flat shell element. The stiffeners are modeled as three-node isoparametric beam elements based on Timoshenko beam theory. Bilinear in-plane displacement constraints are used to maintain the inter-layer continuity. A special lumping technique is used in deriving the lumped mass matrices. The natural frequencies are extracted using the subspace iteration method. Numerical results are presented for unstiffened laminated plates, stiffened isotropic plates, stiffened symmetric angle-ply laminates, stiffened skew-symmetric angle-ply laminates and stiffened skew-symmetric cross-ply laminates. The effects of fiber orientations (ply angles), number of layers, stiffener depths and degrees of orthotropy are examined.

Key words: finite element method; free vibration; frequency; stiffened plates; laminated plates; composite; layered model.

1. Introduction

The application of laminated fiber reinforced composites as structural plate elements or members has been steadily increasing in the field of civil, aerospace, mechanical and marine structures, etc. This is mainly due to their high specific strength and high specific stiffness, which can be tailored by varying the fiber orientation, stacking sequence, etc. Further increase in specific strength and

[†] Senior Bridge Engineer

[‡] Chair and Raymond-Blythe Professor

^{‡†} Tepin Professor of Structural Engineering

stiffness can be achieved by stiffening the laminated plates. Stiffeners in the form of thin elements or solid cross sections are often used to construct the stiffened plated systems. These stiffeners are usually placed along the major load carrying directions. However, the analysis of stiffened laminated plate structures becomes more complicated than that of non-stiffened ones due to the plate-stiffened interaction.

Dynamic analysis is an important issue of the structural investigation and design. Determining the free vibration characteristics of a structural system often appears to be the fundamental task in dynamic analysis. Many researchers have investigated the free vibration of laminated plates in the past. But published works on the dynamic analysis of stiffened laminated plate structures are still scarce in the literature. Based on classical plate theory, early investigations on the free vibration of stiffened plates were performed by Lin (1960) and Wah (1964). Lin's solution was based on analytical method whereas Wah's was a numerical (finite difference) technique. Chao and Lee (1980) adopted the classical laminate theory and the stiffener-plate coupling was treated based on the equivalent orthotropic idealization. The extensional displacements in the laminate were assumed to be uniform and the shear lag effect was neglected. The stiffeners were then treated as elastic supports for the laminated plate. Harik and Guo (1993) developed a semi-discrete plate-beam finite element solution for the free vibration of eccentrically stiffened plates. In their semi-discrete model, an equivalent orthotropic plate analogy was employed to account for the plate-stiffener interaction, but the stiffeners were modeled by beam element. Ataaf and Hollaway (1990) carried out vibration analysis of stiffened and unstiffened composite plates subjected to in-plane loads. Lee and Lee (1995) conducted vibration analysis of anisotropic plates with eccentric stiffeners. Ghosh and Biswal (1996) performed free vibration analysis of stiffened laminated plates using higher-order shear deformation theory. Kolli and Chandrashekara (1997) conducted nonlinear static and dynamic analysis of stiffened laminated plates using 9-node quadratic elements and 3-node beam elements along with transverse shear deformation effects. Lateral strain effects are also incorporated for the stiffener.

In most of the complete finite element free vibration analyses on stiffened laminated plate structures, the plate and stiffener(s) were idealized as separate entities (discrete plate-beam model). The plate and the stiffener(s) were assembled together afterwards in the light of the displacement compatibility along the plate-stiffener interface. The extensional deformation was often represented using independent degrees of freedom in the plate and beam elements. For laminated composite plates, the classical laminate theory is implemented in the early investigations. The classical laminate theory is adequate for many engineering problems. However, the laminates made of typical filamentary composite materials, like graphite-epoxy, are susceptible to the thickness effect because their shear modulus are significantly smaller than their Young's modulus in the fiber direction. The high ratio of Young's modulus to shear modulus renders the classical laminate theory inadequate for analysis of composite plates. The first order shear deformable plate theory (FSDT) introduces a transverse shear deformation with linear variation in the thickness direction (constant transverse shear strains). Similarly, a laminate is treated as an equivalent single layer plate and the FSDT is applied to the analysis of laminated plates/shells. In such a way, the shear correction factor must be properly evaluated in order to represent the actual parabolic distribution of transverse shear deformation along the thickness direction in terms of a linear one. By the nature of the FSDT, the traction free condition at the plate surfaces cannot be satisfied. To overcome the drawbacks of the FSDT, the refined shear deformable plate models, including higher order deformable models, layered (zigzag) models and 3-D elasticity models have been developed. A dynamics formulation of

geometrically-exact sandwich shells for multilayered structures has been developed more recently by Vu-Quoc *et al.* (2001).

In this paper, a layered (zigzag) finite element formulation is developed for the free vibration analysis of stiffened laminated composite plates. The laminated plate is discretized into layers in the thickness direction. The degenerated nine-node isoparametric shell elements are used to represent each layer, while the stiffeners are discretized into three-node isoparametric beam elements. Instead of using the conventional linear constraints, bilinear constraints are applied to retain the independent transverse shear deformations in both layers adjacent to the interface. The plate-stiffener interaction can be considered. A special lumping technique is adopted to derive the lumped mass matrices for both the shell element and beam elements. The eigenvalues are extracted by the subspace iteration method. Extensive numerical examples are given to verify the applicability of current formulation.

2. Layered finite element formulation

A typical stiffened laminated plate with stiffeners along x and y -direction is shown in Fig. 1. Modeling of laminated plates based on the present formulation requires discretization in the thickness direction (z -mesh) in addition to the discretization in the plate plane (x - y mesh). Thus, the in-plane mesh divides the laminate/plate into element stacks and the z -mesh subdivides each element stack into overlaid shell elements. The term “layer” here denotes a discretized finite element layer. A physical layer (lamina) in a laminated plate is always discretized as a layer, but an unlaminated plate is either handled as one layer or subdivided into several layers.

It is assumed that the laminate is built by a number of laminae perfectly bonded together. There are no relative displacements at the laminate-stiffener interfaces. The deformations in any layer is assumed to follow the Mindlin hypothesis, i.e., a straight line element perpendicular to the middle

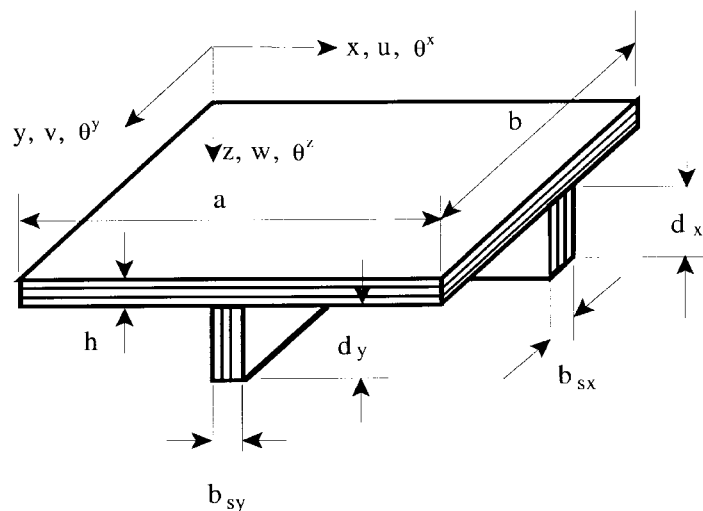


Fig. 1 A typical stiffened laminated plate

plane before bending remains straight during bending, but does not necessarily remain normal to the neutral surface of the layer. However, the transverse shear deformations in adjacent layers are not necessarily equal. The effect of transverse normal stress is neglected in the element formulation. The transverse normal strain is assumed to be negligible. As a result the transverse deflections along a normal line are identical. The stiffeners are assumed to have a rectangular cross section, and the contribution of warping is not considered. The stiffeners can also be laminated. The free vibration of an undamped structural system results into an eigenvalue problem. In finite element matrix form, the generalized eigen problem can be expressed as:

$$[[K] - \omega^2[M]]\{\Delta\} = \{0\} \quad (1)$$

where $[K]$ is the global stiffness matrix; ω is the undamped natural frequency; $[M]$ is the global mass matrix; and $\{\Delta\}$ is the global modal displacement vector. They are generated through the assembly of the element matrices.

2.1 Element stiffness matrices

A degenerated nine-node rectangular isoparametric shell element having uniform thickness along with its natural coordinates, as shown in Fig. 2, is applied to the layers of laminated composite plate. The x - y plane is parallel to the element middle plane and the natural coordinates r and s are parallel to the x and y axes. The shape functions for the element geometry follows the Lagrangian interpolation (Bathe 1982). A 3-node isoparametric beam element with all six DOFs, as shown in Fig. 3, is used to model the stiffeners. Since there is no substantial difference in the formulation of isoparametric shell element and beam element, the derivation presented here is applicable to both the element types.

The displacement components at any point in an element can be represented by the element nodal displacements as follows

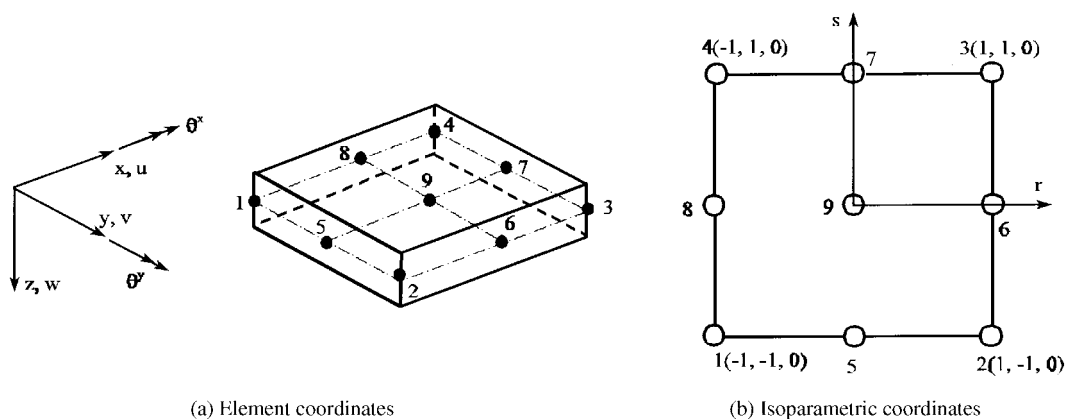


Fig. 2 A degenerated nine-node isoparametric shell element

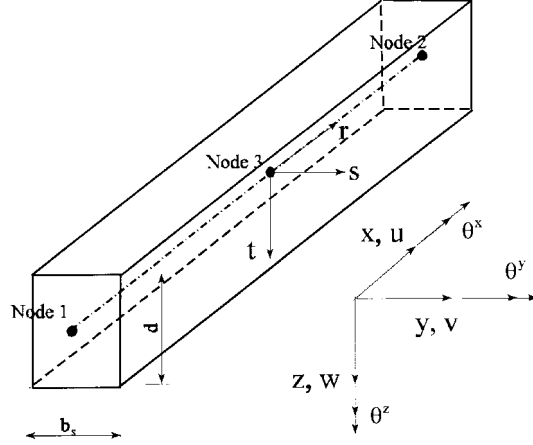


Fig. 3 A straight prismatic 3-D isoparametric beam element

$$(u \ v \ w)^T = \sum_{k=1}^9 [H_k] \{\delta_k^e\} \tag{2}$$

where $\{\delta_k^e\} = [u_k \ v_k \ w_k \ 2_k^x \ 2_k^y]^T$ is the nodal displacement vector of the shell element (for beam element $\{\delta_k^e\} = [u_k \ v_k \ w_k \ 2_k^x \ 2_k^y \ 2_k^z]^T$); and $[H_k]$ is the generalized shape function matrix. The shape function matrix can be written as

$$[H_k] = N_k(r, s)([I][P]) \tag{3}$$

where $N_k(r, s)$ is the shape function; $[I]$ is the identity matrix of size 3×3 ; and the matrix $[P]$ can be defined for the shell and beam elements as

$$[P] = t \frac{h_L}{2} \begin{bmatrix} 0 & 1 \\ -1 & 0 \\ 0 & 0 \end{bmatrix} \text{ (for shell element)} \tag{4}$$

$$[P] = \begin{bmatrix} 0 & t \frac{d}{2} & -s \frac{b_s}{2} \\ -t \frac{d}{2} & 0 & 0 \\ 0 & 0 & 0 \end{bmatrix} \text{ (for x-stiffener); } [P] = \begin{bmatrix} 0 & t \frac{d}{2} & 0 \\ -t \frac{d}{2} & 0 & -s \frac{b_s}{2} \\ 0 & 0 & 0 \end{bmatrix} \text{ (for y-stiffener)} \tag{5}$$

where d and b_s are the depth and breadth of the stiffener; h_L is the thickness of shell element in layer L as shown in Fig. 4; and t is the natural coordinate with respect to plate thickness.

The strain-displacement relationship in matrix form can be written as

$$\{\epsilon^*\} = \sum_{k=1}^{nen} [B_k] \{\delta_k^e\} \tag{6}$$

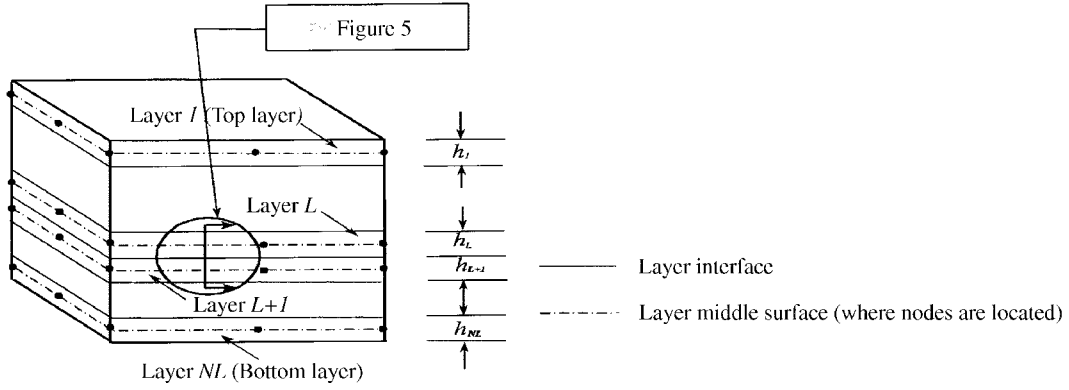


Fig. 4 Element stack and mesh in thickness direction

where nen is the number of nodes per element ($nen = 9$ for the shell element and 3 for the beam element); $\{\varepsilon^*\} = (\varepsilon_{xx} \ \varepsilon_{yy} \ 2\varepsilon_{yz} \ 2\varepsilon_{zx} \ 2\varepsilon_{xy})^T$ and $[B_k]$ is a submatrix of the strain-displacement matrix $[B]$. The submatrix of $[B]$ can be expressed as

$$[B_k] = [B_{k1} \dots B_{k5}]^T \tag{7}$$

$$[B_{k1}] = J_{11}^{-1} \frac{\partial [H_k^{(1)}]}{\partial r} \tag{8a}$$

$$[B_{k2}] = J_{22}^{-1} \frac{\partial [H_k^{(2)}]}{\partial s} \tag{8b}$$

$$[B_{k3}] = J_{22}^{-1} \frac{\partial [H_k^{(3)}]}{\partial s} + J_{33}^{-1} \frac{\partial [H_k^{(2)}]}{\partial t} \tag{8c}$$

$$[B_{k4}] = J_{11}^{-1} \frac{\partial [H_k^{(3)}]}{\partial r} + J_{33}^{-1} \frac{\partial [H_k^{(1)}]}{\partial t} \tag{8d}$$

$$[B_{k5}] = J_{22}^{-1} \frac{\partial [H_k^{(1)}]}{\partial s} + J_{11}^{-1} \frac{\partial [H_k^{(2)}]}{\partial r} \tag{8e}$$

where $[H_k^{(1)}]$ is the submatrix representing the first row of $[H_k]$, and so on. The Jacobian matrices for the shell and beam elements are obtained as

$$[J] = \begin{bmatrix} \frac{\partial x}{\partial r} & \frac{\partial y}{\partial r} & \frac{\partial z}{\partial r} \\ \frac{\partial x}{\partial s} & \frac{\partial y}{\partial s} & \frac{\partial z}{\partial s} \\ \frac{\partial x}{\partial t} & \frac{\partial y}{\partial t} & \frac{\partial z}{\partial t} \end{bmatrix} = \begin{bmatrix} \frac{l_x}{2} & 0 & 0 \\ 0 & \frac{l_y}{2} & 0 \\ 0 & 0 & \frac{h_L}{2} \end{bmatrix} \quad (\text{for shell element}) \tag{9}$$

$$[J] = \begin{bmatrix} \frac{l_e}{2} & 0 & 0 \\ 0 & \frac{b_s}{2} & 0 \\ 0 & 0 & \frac{d}{2} \end{bmatrix} \text{ (for } x\text{-stiffener); } [J] = \begin{bmatrix} \frac{b_s}{2} & 0 & 0 \\ 0 & \frac{l_e}{2} & 0 \\ 0 & 0 & \frac{d}{2} \end{bmatrix} \text{ (for } y\text{-stiffener)} \quad (10)$$

where l_x and l_y are the element lengths along x and y -directions, respectively. The element stiffness matrix can be obtained from the energy principle as

$$[K^e] = \int_{-1}^1 \int_{-1}^1 \int_{-1}^1 [B]^T [D] [B] \det(J) dr ds dt \quad (11a)$$

in which $[B] = [B_1 B_{2_1} \dots B_{nen}]$ is the strain-displacement matrix and its submatrices are defined earlier in Eqs. (8a-e). The matrix $[D]$ is known as the material stiffness matrix defined with respect to the local coordinates. The elements of material matrix $[D]$ depend on the material properties of layer and fiber orientation (ply-angle) where

$$[D] = \begin{bmatrix} E_1 & -\nu_{21} & 0 & 0 & 0 \\ -\nu_{12} & E_2 & 0 & 0 & 0 \\ 0 & 0 & G_{23} & 0 & 0 \\ 0 & 0 & 0 & G_{31} & 0 \\ 0 & 0 & 0 & 0 & G_{12} \end{bmatrix} \quad (11b)$$

Expanding Eq. (11a) and noticing that $\det(J) = V_e/8$ for the specific element geometry leads to the submatrix of the stiffness matrix $[K]$:

$$[K_{ij}^e] = \frac{V_e}{8} \int_{-1}^1 \int_{-1}^1 \int_{-1}^1 [B_i]^T [D] [B_j] dr ds dt \text{ (for } i, j = 1, 2, \dots, nen) \quad (12)$$

where V_e is the element volume ($V_e = l_x l_y h_L$ for a shell element, whereas $V_e = l_e b_s d$ for a beam element).

2.2 Interlayer connectivity

The finite element model often does not assign the nodes at the top and bottom surfaces of shell and beam elements. This means that there are no common nodes shared by adjacent element layers. Thus, in order to maintain the in-plane interlayer displacement continuity, restraints must be imposed. In this section, the interface constraints between two adjacent element layers are first constructed. These constraint relations are then extended to the laminated plate-stiffener interface.

An element stack is constructed which is made up of all the element layers in the thickness

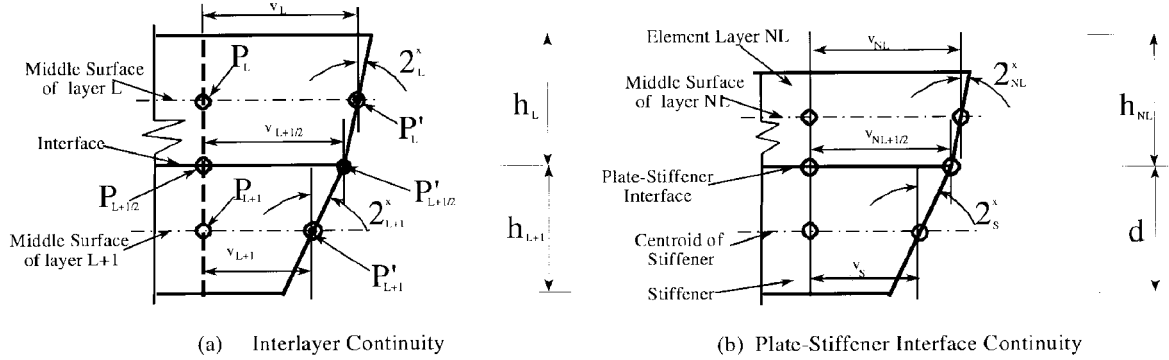


Fig. 5 Bilinear interlayer continuity and plate-stiffener continuity

direction plus the beam element, if any. Since the displacements in a stack are all coupled after the interface constraints are applied, the column heights that determine the skyline of the global stiffness matrix are calculated in terms of element stacks instead of individual elements. The constraints between layers L and $L+1$ are imposed in terms of the displacement at the reference point $P_{L+1/2}$, which is the projection of the nodal points P_L and P_{L+1} on the interface as shown in Fig. 5(a). After deformation, the new locations of points P_L , $P_{L+1/2}$ and P_{L+1} are denoted by P'_L , $P'_{L+1/2}$ and P'_{L+1} . The in-plane displacement $v_{L+1/2}$ at the reference point $P'_{L+1/2}$ can be expressed as:

$$v_{L+1/2} = v_L - \frac{h_L}{2} \theta_L^x \quad (\text{from the upper layer } L, L = 1, 2, \dots, NL - 1) \quad (13)$$

$$v_{L+1/2} = v_{L+1} - \frac{h_{L+1}}{2} \theta_{L+1}^x \quad (\text{from the lower layer } L+1, L = 1, 2, \dots, NL - 1) \quad (14)$$

where NL is the number of element layers excluding the beam layer. Due to the assumption that there is no slip between adjacent layers, Eqs. (13) and (14) must yield a unique quantity. Thus, the interlayer constraint relation for the in-plane displacement v is obtained as:

$$v_L - \frac{h_L}{2} \theta_L^x = v_{L+1} - \frac{h_{L+1}}{2} \theta_{L+1}^x \quad (\text{for } L = 1, 2, \dots, NL - 1) \quad (15)$$

where h_L and h_{L+1} are the thicknesses of the elements in layer L and $L+1$, respectively.

The interlayer constraint relation for in-plane displacement u can be derived as in the same way:

$$u_L + \frac{h_L}{2} \theta_L^y = u_{L+1} - \frac{h_{L+1}}{2} \theta_{L+1}^y \quad (\text{for } L = 1, 2, \dots, NL - 1) \quad (16)$$

In order to eliminate the rotations in layer $L+1$, Eqs. (15) and (16) are rearranged into:

$$\theta_{L+1}^y = (u_{L+1} - u_L) \frac{2}{h_{L+1}} - \theta_L^y \frac{h_L}{h_{L+1}} \quad (\text{for } L = 1, 2, \dots, NL - 1) \quad (17)$$

$$\theta_{L+1}^x = -(v_{L+1} - v_L) \frac{2}{h_{L+1}} - \theta_L^x \frac{h_L}{h_{L+1}} \quad (\text{for } L = 1, 2, \dots, NL - 1) \quad (18)$$

Eqs. (17) and (18) refer to the nodal displacements in two adjacent element layers. The implementation of these constraints cannot be done at the element level. It has to be carried out when the global stiffness matrix is being established. Applying Eqs. (17) and (18) to an element stack layer by layer from the bottom to the top ($L = NL$ to 1) is equivalent to a matrix transformation eliminating all the rotations θ^x and θ^y except those in the top layer. A transformation matrix can be derived from Eqs. (17) and (18) to represent these constraints. However, it is more intuitive to apply them layer by layer.

The constraint equations are also valid for the inter-element connection at the plate-stiffener interface as shown in Fig. 5(b). In this case, L equals NL , layer $L+1$ ($= NL+1$) denotes the beam layer, and h_{L+1} is replaced by the depth of stiffener d . At the nodes where different stiffeners intersect, the stiffener depths in the x and the y -directions are given the corresponding stiffener depths d_x and d_y , respectively.

2.3 Element mass matrix

In current formulation, the mass matrix is derived by considering the kinetic energy due to translational velocities. The effect of rotational velocities on the kinetic energy is neglected. The element mass matrices of the shell and beam elements are lumped to reduce the computational time in extracting the eigenpairs. Three lumping techniques are available in the literature for deriving the lumped element mass matrices: nodal quadrature, row sum and special lumping. For nine-noded rectangular elements, these three methods lead to the same mass matrix (Zienkiewicz 1977). Although there is no mathematical support for the special lumping technique, it is the only method recommended for an arbitrary element since it does not yield negative mass coefficients that vitiate the true solution (Hughes 1987). Therefore, the present work adopts the special lumping technique to derive the lumped mass matrix.

By the special lumping technique, the lumped element mass matrix is obtained by scaling the diagonal mass coefficients of the consistent mass matrix, while the off-diagonal mass coefficients are simply discarded. The summation of the mass coefficients for all the nodes in an element, corresponding to each translation displacement, matches the total element mass. The lumped mass coefficient for each translation DOF at node i can be obtained as:

$$m_{ii} = \alpha \rho V_e \iiint N_i^2 \det(J) dr ds dt \quad (\text{for } i = 1, 2, \dots, nen) \tag{19}$$

where ρ = mass density of the element and α can be defined as

$$\alpha = \frac{1}{\sum_{n=1}^{nen} \iiint N_k^2 \det(J) dr ds dt} \tag{20}$$

Since the present formulation adopts a flat shell element with rectangular shape and uniform thickness, the determinants of the Jacobian matrix in the numerator of Eq. (19) and the denominator of Eq. (20) are constant and can be cancel each other. Thus, the lumped element mass coefficients can be determined by:

$$m_{ii} = \alpha \rho V_e \int_{-1}^1 \int_{-1}^1 N_i^2 dr ds \quad (i = 1, 2, \dots, 9) \quad (21)$$

$$\alpha = \frac{1}{\sum_{k=1}^9 \int_{-1}^1 \int_{-1}^1 N_k^2 dr ds} \quad (22)$$

The integrations in Eqs. (21) and (22) are carried out analytically. The resulting mass coefficients for the shell element corresponding to each translation DOF are: $m_{ii} = \Delta V_e/36$ for the four corner nodes ($i = 1, 2, 3,$ and 4); $m_{ii} = \Delta V_e/9$ for the four midside nodes ($i = 5, 6, 7,$ and 8), and $4\Delta V_e/9$ for the center. The mass coefficients of the beam element can be obtained in a similar way. The assemblage of element matrices follows the skyline procedure.

3. Numerical examples

Extensive numerical examples of free vibration are presented to verify the applicability and accuracy of current layered finite element formulation. These numerical examples include the unstiffened symmetric angle-ply laminates and cross-ply laminates, stiffened isotropic plates, stiffened symmetric angle-ply laminated plate, stiffened skew-symmetric angle-ply, and stiffened skew-symmetric cross-ply laminate. In all the numerical examples, the layer thickness of each layer of an element is assumed to be identical. The material strong (fiber) direction in a stiffener is assumed to coincide with the longitudinal direction of the stiffener. The material properties are given with respect to the laminar coordinates, where 1-direction is along the fiber; 3-direction is normal to the lamina; and 2-direction is orthogonal to direction 1 and 3. The subspace iteration technique (Bathe 1982) is used to extract the eigenvalues and the corresponding eigenvectors.

3.1 Unstiffened symmetric angle-ply laminate

The free vibration of a simply supported square symmetric angle-ply composite laminated plate is analyzed. The material used is E-glass/epoxy with moduli ratios: $E_1/E_2 = 2.45$, $G_{12}/E_2 = G_{31}/E_2 = G_{23}/E_2 = 0.48$ and $\nu_{12} = 0.23$. Natural frequencies corresponding to modes 1, 2, 4, 6, and 8 are obtained and compared with solutions based on classical laminate theory (CLT) by Leissa and Narita (1989). Since the CLT solution is independent of the laminate length to thickness ratio h/a , no explicit h/a value was specified in Leissa and Narita's study. In the present investigation $h/a = 0.01$ is used to comply with the conditions implied in the previous investigation where transverse shear deformation is negligible. The nondimensionalized natural frequencies ($\Omega = \omega a^2 \sqrt{\rho h / D_o}$) are summarized in Table 1, where $D_o = c_{11} h^3 / 12$, $c_{11} = E_1 / (1 - \nu_{12} \nu_{21})$, and $\nu_{21} = \nu_{12} E_2 / E_1$. A good agreement has been found with Leissa and Narita (1989). It is interesting to note that the influence of the ply angle on the natural frequencies varies from mode to mode. The frequency of 6th mode reaches its peak value as θ approaches 15° , but that for other modes at ply angle $\theta = 45^\circ$.

3.2 Unstiffened cross-ply laminates

A simply supported cross-ply square laminated plate with $a/h = 5$ is analyzed. Both symmetric (3-

Table 1 Natural frequency coefficients $\Omega = \omega a^2 \sqrt{\rho h / D_o}$ of a simply supported symmetric square angle-ply laminate

Ply-Angle θ	Source	Frequency Coefficient Ω				
		Mode Number				
		1	2	4	6	8
0°	Present Study	14.89	33.07	59.36	88.01	105.5
	Leissa and Narita (1989)	15.19	33.31	60.78	90.31	108.7
15°	Present Study	15.07	33.34	59.69	88.79	107.1
	Leissa and Narita (1989)	15.37	34.03	60.80	91.40	108.9
30°	Present Study	15.36	35.24	60.49	85.67	107.2
	Leissa and Narita (1989)	15.86	35.77	61.27	85.67	108.9
45°	Present Study	15.78	36.01	61.05	79.19	107.0
	Leissa and Narita (1989)	16.08	36.83	61.65	79.74	109.0

Table 2 Fundamental frequency coefficients $\Omega = \omega h \sqrt{\rho / E_2}$ of a simple supported cross-ply laminated square plate

Number of Layers	Source	Fundamental Frequency Coefficient Ω				
		E_1/E_2				
		3	10	20	30	40
2	Present Study	2.50	2.70	3.10	3.27	3.41
	Noor(1973)	2.46	2.81	3.12	3.33	3.49
3	Present Study	2.65	3.28	3.82	4.11	4.30
	Noor(1973)	2.53	3.26	3.75	4.02	4.19

layer) and skew-symmetric (2-layer) lamination schemes are considered. The orthotropic material properties of each lamina are: $G_{12}/E_2 = G_{31}/E_2 = 0.6$, $G_{23}/E_2 = 0.5$ and $\nu_{12} = 0.25$. The fundamental frequencies for $E_1/E_2 = 3, 10, 20, 30$, and 40 are summarized in Table 2 in the form of nondimensional parameter $\Omega = \omega h \sqrt{\rho / E_2}$. The results agree well with Noor (1973) which is based on the 3-D elasticity theory. It can be seen that the two-layer cross-ply laminate yields lower natural frequencies than the three-layer one. The difference decreases as the orthotropic ratio E_1/E_2 approaches unity. This is because, in the three-layer laminate, the two face layers are balanced in stiffness and are able to constitute higher plate rigidity, but for the two layer cross-ply laminate, the material stiffness coefficients of the two layers are distinct in any specific direction. As a result, the neutral surfaces in the x and y -directions do not coincide for the two-layer laminate unless the degree of material orthotropy equals one. This offset in neutral surfaces plus the non-zero Poisson's ratio leads to the bending-stretching coupling.

It is demonstrated that the bending-stretching coupling reduces the effective stiffness of the two layer cross-ply laminate, but its effect decreases as the number of laminae increases. For a laminate with a large number of laminae, this coupling becomes negligible. If a symmetric laminate is made up of many layers, adding a single layer changes the laminate's category from symmetric to antisymmetric. Two different neutral surfaces with respect to the bending about the x and y -axes

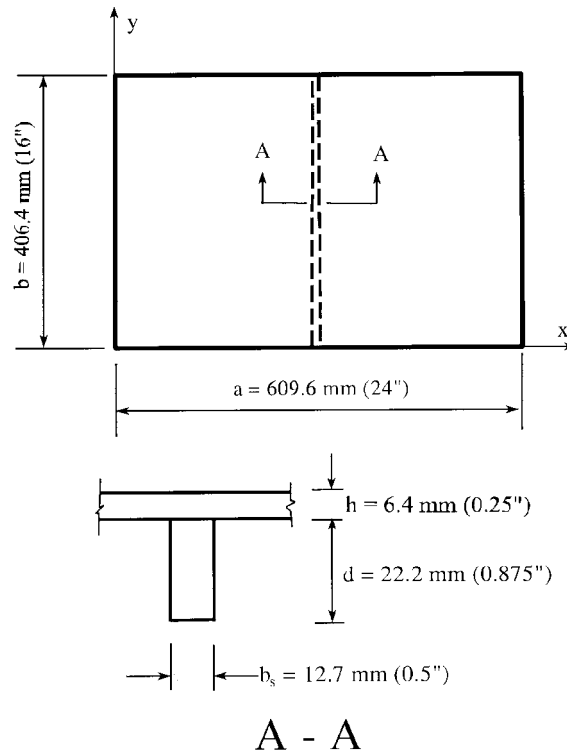


Fig. 6 A simply supported stiffened isotropic plate

Table 3 Natural frequencies (Hz) of a simply supported stiffened isotropic rectangular plate

Mode Number	Natural Frequency (Hz)				
	Aksu (1982)	Bhimaraddi <i>et al.</i> (1989)		Harik and Guo (1993)	Present Study
		CPT	FSDT		
1	254.94	250.27	247.83	253.59	250.26
2	269.46	274.49	274.14	282.02	263.97
3	511.64	517.77	513.63	513.50	526.77

CPT = classical plate theory ; FSDT = first order shear deformable theory

appear. However, logically, the offset between these two neutral surfaces due to the extra layer should be very small. As a result, the coupling effect should be small too.

3.3 Stiffened isotropic plates

The free vibration of a simply supported stiffened rectangular isotropic plate, as shown in Fig. 6, is investigated using the proposed formulation. The stiffener is located at the center along y -direction. The material properties of the plate and stiffener are: Young's modulus $E = 207 \text{ GPa}$ ($30 \times 10^3 \text{ ksi}$),

Poisson's ratio $\nu = 0.3$ and density $\rho = 7830 \text{ kg/m}^3$ (489 lb/ft³). The first three natural frequencies are summarized in Table 3 and compared with Aksu (1982), Bhimaraddi *et al.* (1989), Harik and Guo (1993). A good agreement has been found. Aksu (1982) initially solved this problem using the finite difference method based on the classical plate theory. Bhimaraddi *et al.* (1989) presented finite element solutions based on the first order shear deformable plate theory. Harik and Guo (1993) studied the same problem using a semi discrete plate-beam finite element model.

The example plate is in fact a thin plate ($b/h = 609.6/6.4 = 95$). Thus, a single layer model is used since the transverse shear deformations are insignificant for such a plate. The fundamental frequency from the present study is the second lowest when compared with the other solutions, while the frequencies for mode 2 and mode 3 are comparatively the lowest and highest, respectively. This difference could be attributed to the solution procedure itself. According to the Sturm Sequence properties of eigenvalue problems (Bathe 1982), as the number of eigenpairs included in the matrix iterations increases, the frequencies tend to increase for the higher modes and decrease for the lower modes. In the present study, the number of eigenpairs determined from the subspace iteration is 10 for this problem.

3.4 Stiffened symmetric angle-ply laminated plate

The free vibration of a simply supported stiffened angle-ply square laminated plate with $a/h = 100$, as shown in Fig. 7, is analyzed. A central stiffener is along y -direction. The material (E-glass/Epoxy) properties of the laminate and stiffener are: $E_1/E_2 = 2.45$, $G_{12}/E_2 = G_{31}/E_2 = G_{23}/E_2 = 0.48$, $\nu_{12} = 0.23$. The stiffener is assumed to be constructed from a single layer of material whose strong (fiber) direction is parallel to the stiffener centroidal axis. Natural frequencies are obtained for various ply angles θ , and stiffener depth to thickness ratios d/h . The effects of the stiffener depth and the fiber orientation (ply-angle) on the first and second nondimensional natural frequency $\Omega_1 = \omega_1 a^2 \sqrt{\rho h / D_o}$ are illustrated in Fig. 8a and Fig. 8b respectively. The ply-angles range from 0° to 90° and stiffener depth to laminate thickness ratios vary from 1 to 8. The changes in the modal deflection along the center line in the x -direction for different ply-angles and stiffener depth ratios are also shown in the

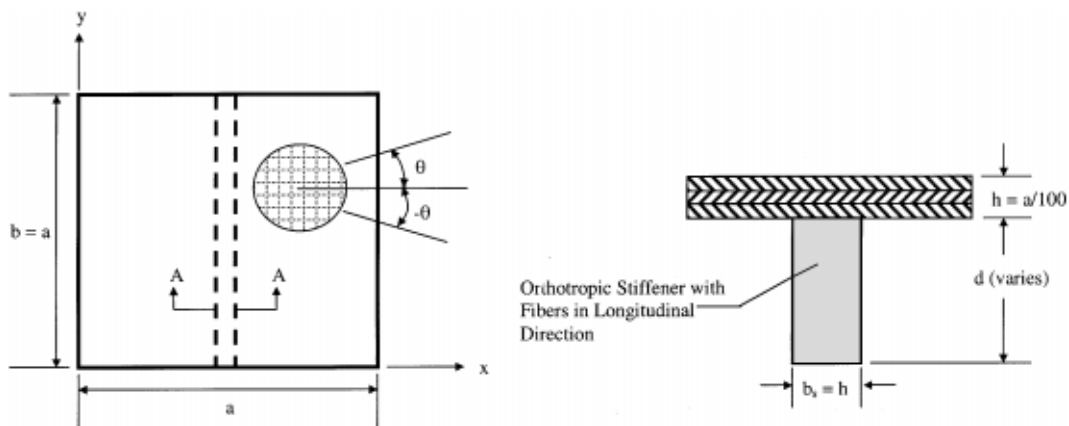


Fig. 7 A simply supported stiffened angle-ply square laminated plate

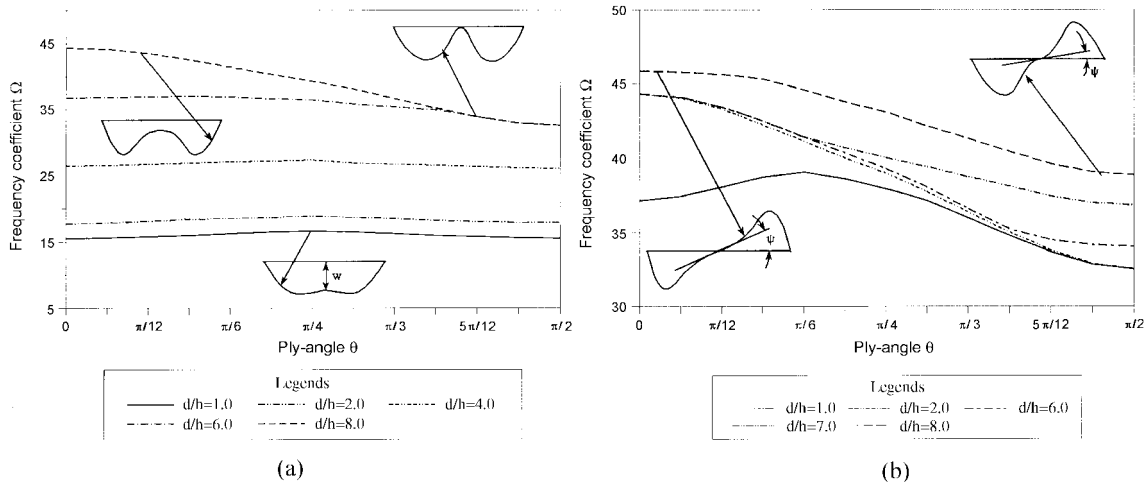


Fig. 8 (a) Nondimensional fundamental frequency variations of a simply stiffened angle-ply laminate, (b) Nondimensional second frequency variations of a simply stiffened angle-ply laminate

figures. The distance across which the modal deflection or rotation is reduced due to the presence of the stiffener is hereunto referred as the influential range of the stiffener. The following observations can be made:

- For a deep stiffener ($d/h > 7$), the natural frequencies decrease as the ply angle increases;
- The fundamental mode shape corresponds to a symmetric mode about the stiffener while the second mode is antisymmetric about the stiffener;
- The modal deflection, w , for the first mode (Fig. 8a) and the modal rotation, P , for the second mode (Fig. 8b) decrease with an increase in the ply-angle;
- The curvature of the mode shape crossing the stiffener increases as the ply-angle increases (Figs. 8a and 8b). On the other hand, the influential range of the stiffener decreases when the angle between the stiffener and the fibers decreases.

All these phenomena are associated with the lower lamina stiffness in the direction perpendicular to the fibers. If lamina were idealized as a collection of combined fibers, the number of fibers crossing the stiffener would decrease as the ply-angle increased. The fibers that do not cross the stiffener are only affected indirectly by the relatively weak lateral linkage among the fibers. On the other hand, the fibers crossing the stiffener enforce the stiffener to undergo torsional deformation. As a result, the more fibers that cross the stiffener, the wider the influential range is and the greater the deflections, w , (Fig. 8a) or the rotations (Fig. 8b) are.

It can be found from the results that a stiffener should be oriented perpendicular to the face layer fiber direction in order to obtain a higher fundamental frequency. Otherwise, the stiffener should be placed at a small angle from the face layer fiber direction if the objective is to reduce the modal deflections at the stiffener location. With regards to the reduction of the rotational vibration at prescribed points, a smaller angle between the face fiber direction and the stiffener results in a smaller rotational magnitude. Unfortunately, this condition also leads to smaller influential ranges.

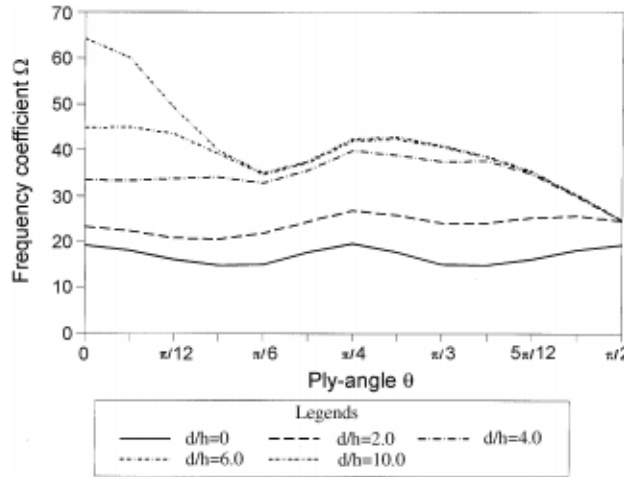


Fig. 9 Fundamental frequency coefficient variations of a simply stiffened angle-ply square laminate

To increase the influential range, the stiffener must be oriented at a larger angle from the face fiber direction. The key issue to decrease the modal rotation along the stiffener is to use a stiffener with a relatively high torsional rigidity.

3.5 Stiffened skew-symmetric angle-ply laminate

A stiffened skew-symmetric angle-ply square composite laminate with $a/h = 100$ and having a central stiffener along y -direction is analyzed in the sense of free vibration. The width of the stiffener is assumed to be equal to the laminate thickness and the material strong direction in the stiffener coincides with the longitudinal axis. The orthotropic material properties for each lamina in the laminate and stiffener are: $E_1/E_2 = 40$, $G_{12}/E_2 = 0.6$, $G_{31}/E_2 = G_{23}/E_2 = 0.5$ and $\nu_{12} = 0.25$. A parametric study was carried out with respect to the stiffener depth ratio d/h and the ply-angle θ .

Fig. 9 gives the variation of the nondimensional frequency coefficient $\Omega = \omega h \sqrt{\rho/E_2}$ versus the ply-angles for various stiffener depths to laminate thickness ratios. It is found that the fundamental frequency coefficients Ω , was 15.03 for $a/h = 5.0$, $\theta = 45^\circ$ and $d/h = 0.01$. The corresponding values for an unstiffened case obtained by Bert and Chen (1978) and Reddy (1979) were 13.04 and 15.71, respectively. Bert and Chen derived an analytical solution based on the first order shear deformable theory (FSDT), and Reddy developed finite element method based on the higher order shear deformable theory (HSDT). The percent difference between the Ω values is low enough to establish confidence in the accuracy of the present results.

For an unstiffened square laminate, it is demonstrated that the laminate with ply-angle $\theta = \alpha$ behaves the same way as the laminate with ply-angle $\theta = 90^\circ - \alpha$. Thus, the $\Omega - \theta$ curve is symmetric about $\theta = 45^\circ$. However, the laminate's behavior is totally different in the stiffened laminate case. For example, the overall stiffness of the laminate is much higher when $\theta = 0^\circ$, since the stiffener is perpendicular to the strong direction of the laminate. From Fig. 9, it can be seen that when the ply-angle approaches 90° , no significant gain in the natural frequency is obtained as the stiffener depth to laminate thickness ratio is increased from 2 to 10. Stiffeners with a depth to plate thickness ratio equal to 2 are substantially strong enough to form an intermediate support, because

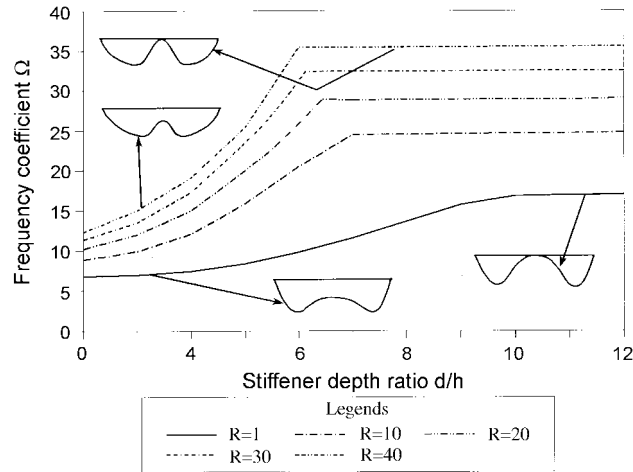


Fig. 10 Fundamental frequency coefficient variations of a simply stiffened cross-ply square laminate

the stiffener has a small influential range as the ply-angle approaches 90° . Therefore, greater stiffener depth does not make much of a difference.

3.6 Stiffened skew-symmetric cross-ply laminate

The free vibration of a stiffened skew-symmetric cross-ply square composite laminated plate with $a/h = 100$ is analyzed. A central stiffener is along y -direction. The width of the stiffener is assumed to be equal to the laminate thickness. The material strong direction in the stiffener coincides with the longitudinal axis. The material properties of each lamina for both plate and stiffener are: $G_{12}/E_2 = 0.6$, $G_{31}/E_2 = G_{23}/E_2 = 0.5$, and $\nu_{12} = 0.25$. A parametric study is conducted with stiffener depth to laminate thickness ratios, d/h , varying from 0.01 to 12 and degree of orthotropy, $R (= E_1/E_2)$, equal to 1, 10, 20, 30, and 40.

From the analysis, the nondimensional fundamental frequency coefficients $\Omega = \omega h \sqrt{\rho/E_2}$ are obtained. The results are plotted in Fig. 10. For a given stiffener depth to laminate thickness ratio d/h , it is demonstrated that the frequency coefficient increases as the degree of orthotropy (R) increases. However, for each degree of orthotropy, the fundamental frequency reaches an upper limit as the stiffener depth to laminate thickness ratio d/h reaches a certain value. By examining the mode shape, it is observed that the modal deflection along the stiffener is zero after the frequency reaches the upper limit. This limit indicates that the stiffener acts as an intermediate support when it is sufficiently deep.

It is interesting to note that the higher the degree of orthotropy, the sooner the frequency coefficient approaches its upper limit. The transverse stiffness of the laminate determines how much the stiffener can influence the mode shape. As the degree of orthotropy increases, the transverse stiffness of the laminate becomes relatively lower. Consequently, the influential range of the stiffener is also reduced. Thus, the intermediate support resembles more of a simple support for higher degrees of orthotropy, while it is a fixed edge for an isotropic plate. In other words, for a given stiffener depth to laminate thickness ratio d/h , if the laminate has a high degree of orthotropy, then the stiffener possesses a narrower influential range.

4. Conclusions

The development of a layered (zigzag) finite element model for the free vibration analysis of stiffened laminated composite plates is presented. Nine-node degenerated isoparametric shell element is used to model each layer and 3-D beam element is adopted to model the stiffener. Bilinear in-plane displacement constraints are used to maintain the inter-layer continuity of the stiffened laminated plate. Element lumped mass matrices are derived based on a special lumping technique. Using the present finite element model, free vibration results are presented for unstiffened laminated plates, stiffened isotropic plates, stiffened symmetric angle-ply laminates, stiffened skew-symmetric angle-ply laminates and stiffened skew-symmetric cross-ply laminates. The influence of different ply angles, number of layers, number of stiffeners, stiffener depth and degree of orthotropy on the natural frequencies are studied.

Comparisons with available solutions have shown that the proposed finite element model is superior in accuracy to the equivalent single layer models and also can compete with the higher order shear deformable models in modeling the thin laminates. It is observed that the influence of the ply angle on the natural frequencies varies from mode to mode. The bending-stretching coupling is found to reduce the effective stiffness of the two layer cross-ply laminate, but its effect decreases as the number of laminae increases. For a laminate with a large number of laminae, this coupling becomes negligible. It is also seen that the stiffener should be oriented perpendicular to the face layer fiber direction in order to obtain a higher fundamental frequency.

References

- Aksu, G. (1982), "Free vibration analysis of stiffened plates including the in-plane inertia," *J. Appl. Mech.*, **49**, 206-212.
- Ataaf and Hollaway (1990), "Vibrational analyses of stiffened and unstiffened composite plates subjected to in-plane loads," *Composites*, **21**(2), 117-126.
- Bathe, K.J. (1982), *Finite Element Procedures in Engineering Analysis*, Prentice-Hall, Englewood Cliffs, New Jersey.
- Bert, C.W. and Chen, T.L.C. (1978), "Effect of shear deformation on vibration of antisymmetric angle-ply laminated rectangular plates," *Int. J. Solids Struct.*, **14**(6), 465-473.
- Bhimaraddi, A., Carr, A.J. and Moss, P.J. (1989), "Finite element analysis of laminated shells of revolution with laminated stiffeners," *Int. J. Comput. Struct.*, **33**(1), 295-305.
- Chao, C.C. and Lee, J.C. (1980), "Vibration of eccentrically stiffened laminates," *J. Composite Materials*, **14**, 233-244.
- Ghosh, A.K. and Biswal, K.C. (1996), "Free-vibration analysis of stiffened laminated plates using higher-order shear deformation theory," *Finite Elements in Analysis and Design*, **22**, 143-161.
- Harik, I.E. and Guo, M.-W. (1993), "Finite element analysis of eccentrically stiffened plates in free vibration," *Int. J. Comput. Struct.*, **49**, 1007-1015.
- Hughes, T.J.R. (1987), *The Finite Element Method, Linear Static and Dynamic Finite Element Analysis*, Prentice-Hall, Englewood Cliffs, New Jersey.
- Kolli, M. and Chandrashekhara, K. (1997), "Non-linear static and dynamic analysis of stiffened laminated plates," *Int. J. Non-linear Mechanics*, **32**(1), 89-101.
- Lee, D.-M. and Lee, I. (1995), "Vibration analysis of anisotropic plates with eccentric stiffeners," *Comput. Struct.*, **57**(1), 99-105.
- Leissa, A.W. and Narita, Y. (1989), "Vibration studies for simply supported symmetrically laminated rectangular plates," *Compos. Struct.*, **12**, 113-132.

- Lin, Y.K. (1960), "Free vibration of continuous skin-stringer panels," *J. Appl. Mech.*, **27**(4), 669-681.
- Reddy, J.N. (1979), "Free vibration of antisymmetric, angle-ply laminated plates including transverse shear deformation by the finite element method," *J. Sound Vib.*, **66**(4), 565-576.
- Vu-Quoc, L., Deng, H. and Tan, X.G. (2001), "Geometrically-exact sandwich shells; the dynamic case," *Comput. Method. Appl. Mech. Engrg.*, **190**(22-23), 2825-2873
- Wah, T. (1964), "Vibration of stiffened plates," *Aero. Quarterly*, **15**, part-3, 285-298.
- Zienkiewicz, O.C. (1977), *The Finite Element Method-3rd Edition*, McGraw-Hill, England.

Notation

a, b	: plate length in x direction and y direction respectively
b_s	: breadth of stiffener cross section
c_{11}	: $E_1/(1 - \nu_{12} \nu_{21})$, material stiffness coefficient in laminar coordinates
d	: depth of stiffener cross section
D_o	: $c_{11}h^3/12$, laminate flexural rigidity in laminar coordinates
E_1, E_2	: elastic moduli in fibre principle directions
G_{12}, G_{23}, G_{31}	: shear moduli with respect to fiber principle directions
h	: laminate thickness
h_L	: thickness of a plate element in element layer L (Figs. 4 and 5)
r, s, t	: natural coordinates where t is in the direction of normal
u, v, w	: translational displacement in global axis x, y , and z direction
x, y, z	: global (Cartesian) coordinates
θ	: ply-angle, from global x -axis to fiber direction
$\theta^x \theta^y \theta^z$: rotational displacements with respect to the global coordinates
ν_{ij}	: Poisson's ratio, transverse strain in j -direction due to stress